

Significant enhancement in thermoelectric properties of polycrystalline Pr-doped SrTiO_{3-δ} ceramics originating from nonuniform distribution of Pr dopants

Arash Mehdizadeh Dehkordi, Sriparna Bhattacharya, Jian He, Husam N. Alshareef, and Terry M. Tritt

Citation: *Applied Physics Letters* **104**, 193902 (2014); doi: 10.1063/1.4875925

View online: <http://dx.doi.org/10.1063/1.4875925>

View Table of Contents: <http://scitation.aip.org/content/aip/journal/apl/104/19?ver=pdfcov>

Published by the *AIP Publishing*

Articles you may be interested in

[New insights on the synthesis and electronic transport in bulk polycrystalline Pr-doped SrTiO_{3-δ}](#)

J. Appl. Phys. **117**, 055102 (2015); 10.1063/1.4905417

[Resonant distortion of electronic density of states and enhancement of thermoelectric properties of β-Zn₄Sb₃ by Pr doping](#)

J. Appl. Phys. **113**, 124901 (2013); 10.1063/1.4795840

[Enhancement of thermoelectric performance in strontium titanate by praseodymium substitution](#)

J. Appl. Phys. **113**, 053704 (2013); 10.1063/1.4790307

[Thermoelectric properties of nanostructured Si_{1-x}Ge_x and potential for further improvement](#)

J. Appl. Phys. **108**, 124306 (2010); 10.1063/1.3518579

[Two dimensional metallic conductivity in Pr_{1-x}Sr_xMnO₃ antiferromagnets](#)

J. Appl. Phys. **91**, 8275 (2002); 10.1063/1.1452707



You don't still use this cell phone



or this computer



Why are you still using an AFM designed in the 80's?



It is time to upgrade your AFM
Minimum \$20,000 trade-in discount for purchases before August 31st

Asylum Research is today's technology leader in AFM

dropmyoldAFM@oxinst.com



OXFORD
INSTRUMENTS
The Business of Science®

Significant enhancement in thermoelectric properties of polycrystalline Pr-doped $\text{SrTiO}_{3-\delta}$ ceramics originating from nonuniform distribution of Pr dopants

Arash Mehdizadeh Dehkordi,^{1,a)} Sriparna Bhattacharya,² Jian He,² Husam N. Alshareef,³ and Terry M. Tritt^{1,2,b)}

¹Department of Materials Science and Engineering, Clemson University, Clemson, South Carolina 29634, USA

²Department of Physics and Astronomy, Clemson University, Clemson, South Carolina 29634, USA

³Materials Science and Engineering, King Abdullah University of Science and Technology (KAUST), Thuwal 23955-6900, Saudi Arabia

(Received 24 March 2014; accepted 28 April 2014; published online 12 May 2014)

Recently, we have reported a significant enhancement ($>70\%$ at 500°C) in the thermoelectric power factor (PF) of bulk polycrystalline Pr-doped SrTiO_3 ceramics employing a novel synthesis strategy which led to the highest ever reported values of PF among doped polycrystalline SrTiO_3 . It was found that the formation of Pr-rich grain boundary regions gives rise to an enhancement in carrier mobility. In this Letter, we investigate the electronic and thermal transport in $\text{Sr}_{1-x}\text{Pr}_x\text{TiO}_3$ ceramics in order to determine the optimum doping concentration and to evaluate the overall thermoelectric performance. Simultaneous enhancement in the thermoelectric power factor and reduction in thermal conductivity in these samples resulted in more than 30% improvement in the dimensionless thermoelectric figure of merit (ZT) for the whole temperature range over all previously reported maximum values. Maximum ZT value of 0.35 was obtained at 500°C . © 2014 AIP Publishing LLC. [<http://dx.doi.org/10.1063/1.4875925>]

The quest for stable high performance thermoelectric materials for high-temperature applications remains an active area of research. Oxide thermoelectrics were shown to be promising candidates, from stability and cost perspectives to electronic transport capabilities.¹ Among the n-type oxide thermoelectrics, highly doped strontium titanate (STO) has attracted much attention due to its intriguing electronic properties. Tunable electrical conductivity along with a large carrier effective mass and degenerate conduction band, which leads to a large Seebeck coefficient at high carrier concentrations, promises a large thermoelectric power factor. However, a low carrier mobility ($\mu \sim 6 \text{ cm}^2 \text{ V}^{-1} \text{ s}^{-1}$ at 300 K for single crystals)² and a large total thermal conductivity ($\kappa \sim 12 \text{ W m}^{-1} \text{ K}^{-1}$ at 300 K for single crystals)² detrimentally affect the thermoelectric performance which is evaluated by a dimensionless figure of merit, $ZT = \alpha^2 \sigma T / \kappa$, where α is the Seebeck coefficient, σ the electrical conductivity, κ the total thermal conductivity, and T the absolute temperature in Kelvin. Maximum ZT values of 0.27 and 0.17 at 800°C were reported for La-doped and Nb-doped single crystals, respectively,² which need to be further enhanced in order for STO-based oxides to be able to compete with the other high temperature candidates.

The majority of the experimental investigations in order to improve the thermoelectric performance of STO beyond that of the single crystal have focused on the reduction of κ mainly through lattice distortion and mass fluctuation scattering mechanisms. These attempts include: (i) Single- or double-doping of the Sr^{2+} and/or Ti^{4+} sites, which comprise the main efforts with respect to this direction. The maximum

ZT values of 0.36 at 800°C for co-doped $\text{La}_{0.08}\text{Dy}_{0.12}\text{Sr}_{0.8}\text{TiO}_3$ and 0.35 at 730°C for $\text{SrTi}_{0.8}\text{Nb}_{0.2}\text{O}_3$ are the highest previously reported so far for bulk polycrystalline STO ceramics.^{3,4} (ii) Synthesis of natural superlattice Ruddlesden–Popper structures is another attempt to reduce thermal conductivity.⁵ However, it is observed that the detrimental effect of the insulating SrO layers on carrier mobility reduces electrical conductivity, hence it impairs the thermoelectric power factor (herein defined as $PF = \alpha^2 \sigma T$) more significantly than it reduces thermal conductivity.⁶ (iii) Composite engineering is also another strategy which was employed to reduce the thermal conductivity by addition of a nanosized second phase. Inclusion of YSZ nanoparticles and potassium titanate nanowires in Nb-doped STO matrix resulted in maximum ZT values of 0.21 and 0.34 at 630°C , respectively.^{7,8} It is worth mentioning that due to the very small phonon mean free path in SrTiO_3 ($l_{ph} \sim 2 \text{ nm}$ at 300 K for single crystal),⁹ nanostructuring is not a viable option for the improvement of the TE performance of bulk STO ceramics primarily through the reduction of the lattice thermal conductivity.

However, no enhancement strategy has been reported to substantially increase the thermoelectric power factor in these oxides. The reported maximum power factor (PF) values in bulk single- and poly-crystalline STO have been confined to an upper limit of $PF \leq 1.0 \text{ W m}^{-1} \text{ K}^{-1}$. Very recently, we have reported a significant improvement ($>70\%$ over the previously reported maximum at 500°C) in the thermoelectric power factor of bulk polycrystalline SrTiO_3 via *in situ* Pr doping of the grain boundaries using a novel synthesis strategy.¹⁰ The thermoelectric power factor was enhanced over a broad range of temperature and doping concentration with the highest ever reported value of $\sim 1.3 \text{ W m}^{-1} \text{ K}^{-1}$ at

^{a)}amehdiz@g.clemson.edu

^{b)}ttritt@clemson.edu

500 °C. This pronounced enhancement was a result of much improved carrier mobility (\sim by a factor of 2 at room temperature).

In this Letter, we present and discuss the results of our investigations on the electronic and thermal transport in Pr-doped SrTiO₃ ceramics. We show that the simultaneous enhancement in the thermoelectric power factor and reduction in thermal conductivity resulted in a thermoelectric figure of merit of 0.35 at 500 °C. Investigations were performed to determine the optimum doping concentration. The samples exhibit a larger figure of merit than reported in the literature for the whole temperature range under study.

Sr_{1-x}Pr_xTiO₃ powders with $0 < x \leq 0.175$ were prepared using a solid-state reaction process. Stoichiometric amounts of SrCO₃ powder (99.9%; Aldrich), Pr₂O₃ sintered lumps (99.9%; Alfa Aesar), and TiO₂ nanopowder (99.5%; Aldrich) were mixed, cold pressed into pellets and then calcined in air at 1400 °C with intermediate grinding. The calcined pellets were subsequently pulverized into powders using a mortar and pestle. The resulting powders were densified into disks (12.7 mm diameters and 3 mm thick) using spark plasma sintering (SPS) technique (Dr. Sinter Lab, SPS-515 S) under dynamic vacuum at 1400–1500 °C for 5 min. It was found that SPS heating rate can play a crucial role on the modification of the electronic transport by the formation of the Pr-rich grain boundaries.¹⁰ Densities, ρ , of the bulk samples were determined using the Archimedes method and are all higher than 95% of their theoretical values. Thermal diffusivity, d , was measured on the disk samples using a Netzsch LFA 457 MicroFlash system (300–773 K). The specific heat, C_p was measured on a Netzsch differential scanning calorimeter (DSC) 404 C Pegasus system. Thermal conductivity was then calculated from $\kappa = \rho C_p d$. Rectangular bars ($10 \times 2 \times 2$ mm³) were cut from the disks for the measurements of electrical conductivity (σ) and Seebeck coefficient (α). High temperature measurements were performed using an Ulvac-Riko ZEM-3 (300 K to 800 K) system. Carrier concentration of the samples were determined with a Quantum Design PPMS system using five-probe configuration under low (0.5 T) and high (3 T) magnetic fields (10 K to 300 K). All the transport measurements reported for a given composition were performed on the same sample.

Figure 1(a) shows the temperature dependence of electrical conductivity as a function of nominal doping concentration. All the samples exhibit a degenerate semiconducting behavior. It is observed that σ monotonically increases with increasing Pr content up to $x = 0.15$ (shown with red arrow). Sample with $x = 0.15$ possesses the largest electrical conductivity leading to the maximum power factor of $1.32 \text{ W m}^{-1} \text{ K}^{-1}$ at 500 °C, the largest ever reported for either single- or poly-crystalline SrTiO₃ ceramics. However, a further increase in the Pr content up to $x = 0.175$, results in a marked decrease in the electrical conductivity (shown with gray arrow), most likely originating from a reduction in carrier mobility, μ .

Figure 1(b) shows the Seebeck coefficient as a function of temperature. Diffusive-like thermopower (in agreement with the degenerate semiconducting behavior) is observed for all the samples and no sign of minority carrier contribution and bipolar effects are observed. The absolute α

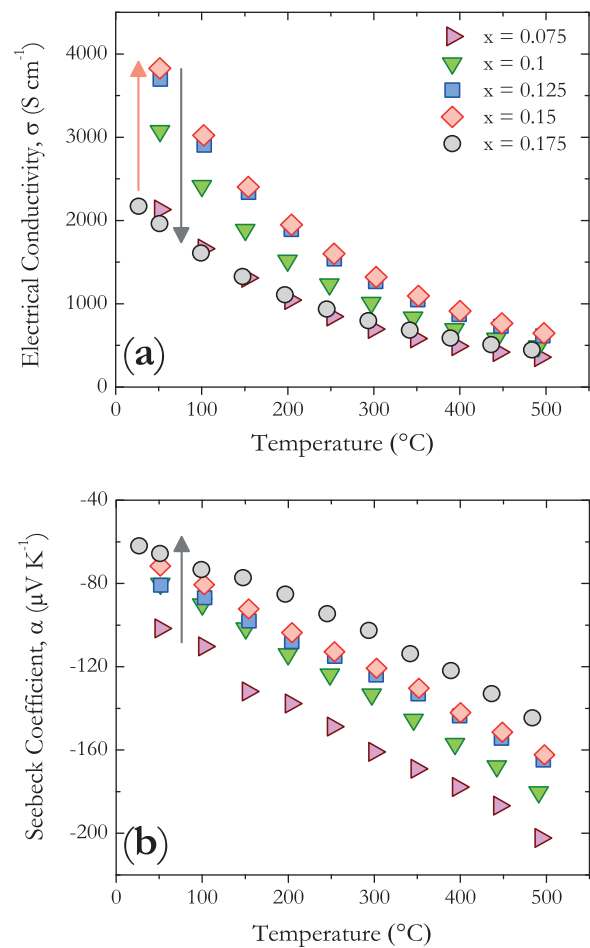


FIG. 1. Temperature dependence in Celsius of (a) electrical conductivity and (b) Seebeck coefficient for Sr_{1-x}Pr_xTiO₃ polycrystalline ceramics as a function of Pr content.

monotonically reduces with increasing the Pr content due to an increase in the carrier concentration, n , which is reported in Table I. However, the increase in the carrier concentration and the corresponding reduction in the absolute thermopower is less pronounced for $x > 0.125$ which suggest the partial incorporation of the Pr dopants in the lattice. Appearance of small peaks of praseodymium oxide in the X-ray diffraction pattern for these samples confirms this suggestion. Room temperature properties are reported in Table I.

Figure 2(a) shows the high-temperature thermal conductivity as a function of temperature and Pr content. It is observed that κ decreases over the whole temperature range with increasing the Pr content for $x \leq 0.15$. Considering the increase in σ with Pr content, this reduction suggests the

TABLE I. Room temperature measured and calculated materials properties.

Sample	Electrical conductivity (S cm ⁻¹)	Seebeck coefficient ($\mu\text{V K}^{-1}$)	Carrier concentration (cm ⁻³)	Mobility (cm ² V ⁻¹ s ⁻¹)	Density (g cm ⁻³)
$x = 0.075$	2740	-92	1.4×10^{21}	12.2	5.21
$x = 0.10$	3535	-76	1.8×10^{21}	12.2	5.24
$x = 0.125$	4135	-75	1.9×10^{21}	13.6	5.27
$x = 0.15$	4365	-67	2.3×10^{21}	11.8	5.31
$x = 0.175$	2170	-62	5.33

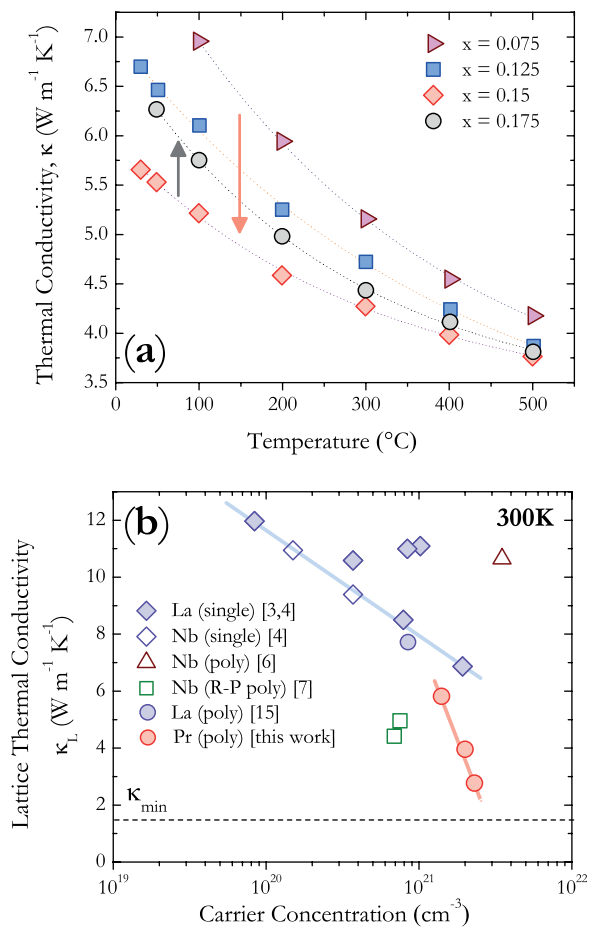


FIG. 2. (a) Temperature dependence in Celsius of total thermal conductivity as a function of Pr content and (b) room temperature lattice thermal conductivity as a function of the carrier concentration for doped single- (single) and polycrystalline (poly) samples. The lines are guides to the eye.

suppression of lattice thermal conductivity with an increase in Pr concentration as well. The lattice thermal conductivity was determined from the Wiedemann-Franz relationship, $\kappa_L = \kappa - \sigma LT$, where σLT is the electronic thermal conductivity and L the Lorenz number for a degenerate semiconductor ($L = 2 \times 10^{-8} \text{ W}\Omega \text{ K}^{-2}$).¹¹ It was found that not only the magnitude of κ_L above room temperature reduces with an increase in the Pr content, but the temperature dependence of κ_L relaxes, from $T^{-0.72}$ for $x=0.05$ to almost temperature-independent for $x=0.15$. Weaker temperature dependence than $1/T$ (i.e., T^{-1}), which is expected for a crystalline material at high temperature, is expected for samples with atomic disorder or other point defects. Further increase in the Pr content of the sample up to $x = 0.175$ leads to an increase in κ as well as κ_L .

In order to further highlight the reduction in κ and the effectiveness of the synthesis strategy employed in this work, the minimum lattice thermal conductivity, κ_{min} , for SrTiO₃ is calculated using Cahill's formula for disordered crystals.^{12,13} The calculated κ_{min} is about $1.5 \text{ W m}^{-1} \text{ K}^{-1}$ at room temperature for pristine SrTiO₃. Figure 2(b) shows the room temperature lattice thermal conductivity as a function of carrier concentration for samples investigated in this work as well as reported in the literature for other single- and poly-crystalline samples. This figure provides a measure of the impact of different dopants on the distortion of the lattice

and its corresponding effect on κ_L . The reported n might possibly include contributions from oxygen vacancies as well which can influence κ_L . However, considering the fact that the measured n are almost always lower than (within 10%) the nominal values, these contributions can be assumed negligible and thus the trends considered valid. A linear decrease in κ_L is observed for La-doped SrTiO₃ single crystals with increasing La content. This reduction originates from the differences in mass ($M_{\text{Sr}} = 87.62 \text{ g mol}^{-1}$ and $M_{\text{La}} = 138.90 \text{ g mol}^{-1}$) and ionic radii ($R_{\text{Sr}^{2+}} = 1.26 \text{ \AA}$, and $R_{\text{La}^{3+}} = 1.16 \text{ \AA}$)¹⁴ of La and Sr which give rise to the mass fluctuation and strain field effect phonon scattering mechanisms. Similar behavior is expected for Pr-doped samples due to the close vicinity of La and Pr in the periodic table and their similar mass ($M_{\text{Pr}} = 140.90 \text{ g mol}^{-1}$) and ionic radius ($R_{\text{Pr}^{3+}} = 1.12 \text{ \AA}$).¹⁴ However, a steep decrease in κ_L was observed with an increase in Pr content of the samples presented in this work. Due to the relatively large average grain size (2–4 μm) in our samples, three orders of magnitude larger than the phonon mean free path, poly-crystalline nature of the ceramics and phonon scattering from the interfaces are not anticipated to play a significant role in the expected trend. In fact, similar values of κ_L achieved for La-doped SrTiO₃ polycrystalline ceramic and its single crystal counterpart attests to this assumption.¹⁵ The significant reduction in κ_L for the non-uniformly Pr-doped SrTiO₃ ceramics suggests the possibility of another phonon scattering mechanism beyond that of mass fluctuation and strain field effect observed in single crystals. X-ray diffraction analysis of the samples supported by electron backscattered diffraction (EBSD) suggests the cubic ($\text{Pm}\bar{3}\text{m}$) to pseudo-cubic ($\text{P4}/\text{mmm}$) transition in the Pr-rich boundary region which is more visible for the samples with $x > 0.125$. This kind of structural transition has been reported in uniformly Pr-doped SrTiO₃ ceramics with $x > 0.05$ which is ascribed to the tilting of the TiO₆ octahedra.^{16,17} This suggests that aside from the respective mass fluctuation and strain field scatterings within the grain and the grain boundary regions, phonons experience an extra strain field-type scattering as they travel from the core domain (grain) to the shell region (Pr-rich grain boundary), comparing to the uniformly doped sample. It is also observed that κ_L for sample with $x=0.15$ is approaching the calculated minimum at room temperature. The knowledge of the phonon dispersion curves and their modification with cubic to tetragonal transition is required to be able to conclusively discuss the phonon scattering mechanisms in these ceramics.

Figure 3 shows the temperature dependence of the figure of merit, ZT. Reported maximum ZT values in the literature for single- and polycrystalline SrTiO₃ are also shown for comparison.^{2–4,8,18,19} Pr-doped SrTiO₃ polycrystalline samples prepared using the strategy employed in this work shows much higher ZT values over the whole temperature range under study. Maximum ZT values above 0.6 can be predicted at 1000 °C by fitting the experimental electronic and thermal transport data, if the measurements are to be performed under a highly reducing atmosphere. Of course, these projections need to be validated experimentally. However, it is worth mentioning that such high ZT values are achieved with high electrical conductivity which makes these

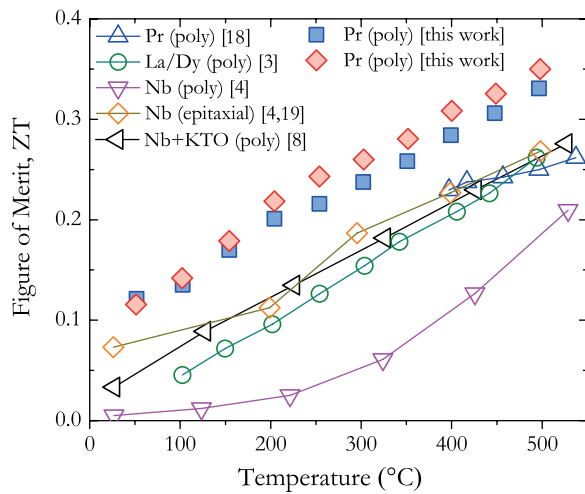


FIG. 3. Temperature dependence of thermoelectric figure of merit, ZT. The lines are guides to the eye.

ceramics desirable candidates for device fabrication due to minimal electrical contact problems.

In summary, the thermoelectric properties of polycrystalline $\text{Sr}_{1-x}\text{Pr}_x\text{TiO}_3$ ceramics were investigated. Results show that a simultaneous enhancement in the thermoelectric power factor and reduction in thermal conductivity was achieved for these samples originating from the nonuniform distribution of dopants from within the grains to the grain boundary region. Optimum nominal Pr concentration of $x = 0.15$ was determined which maximizes the thermoelectric power factor and minimizes the thermal conductivity. Higher ZT values than reported in the literature were achieved over the whole temperature range. A maximum ZT of 0.35 at 500 °C was obtained for this sample.

The authors wish to acknowledge the competitive faculty-initiated collaboration (FIC) grant from KAUST.

- ¹J. He, Y. Liu, and R. Funahashi, *J. Mater. Res.* **26**, 1762 (2011).
- ²S. Ohta, T. Nomura, H. Ohta, and K. Koumoto, *J. Appl. Phys.* **97**, 034106 (2005).
- ³H. Wang, C. Wang, W. Su, J. Liu, Y. Zhao, H. Peng, J. Zhang, M. Zhao, J. Li, N. Yin *et al.*, *Mater. Res. Bull.* **45**, 809 (2010).
- ⁴S. Ohta, H. Ohta, and K. Koumoto, *J. Ceram. Soc. Jpn.* **114**, 102 (2006).
- ⁵Y. Wang, K. H. Lee, H. Ohta, and K. Koumoto, *J. Appl. Phys.* **105**, 103701 (2009).
- ⁶Y. Wang, C. Wan, X. Zhang, L. Shen, K. Koumoto, A. Gupta, and N. Bao, *Appl. Phys. Lett.* **102**, 183905 (2013).
- ⁷N. Wang, H. Li, Y. Ba, Y. Wang, C. Wan, K. Fujinami, and K. Koumoto, *J. Electron. Mater.* **39**, 1777 (2010).
- ⁸N. Wang, H. He, Y. Ba, C. Wan, and K. Koumoto, *J. Ceram. Soc. Jpn.* **118**, 1098 (2010).
- ⁹K. Koumoto, Y. Wang, R. Zhang, A. Kosuga, and R. Funahashi, *Annu. Rev. Mater. Res.* **40**, 363 (2010).
- ¹⁰A. Mehdizadeh Dehkordi, S. Bhattacharya, T. Darroudi, J. W. Graff, U. Schwingenschlöggl, H. N. Alshareef, and T. M. Tritt, *Chem. Mater.* **26**, 2478 (2014).
- ¹¹T. M. Tritt, *Thermal Conductivity: Theory, Properties, and Applications* (Kluwer Academic/Plenum, New York, 2004).
- ¹²D. G. Cahill, S. K. Watson, and R. O. Pohl, *Phys. Rev. B* **46**, 6131 (1992).
- ¹³S. Bhattacharya, A. Mehdizadeh Dehkordi, S. Tennakoon, R. Adebisi, J. Gladden, H. Alshareef, and T. Tritt, "Role of phonon scattering by elastic strain field in thermoelectric $\text{Sr}_{1-x}\text{Y}_x\text{TiO}_3$," *J. Appl. Phys.* (unpublished).
- ¹⁴R. Shannon, *Acta Crystallogr., Sect. A: Cryst. Phys., Diff., Theor. Gen. Crystallogr.* **32**, 751 (1976).
- ¹⁵A. M. Dehkordi, S. Bhattacharya, T. M. Tritt, and H. N. Alshareef, *Bull. Am. Phys. Soc.* **57**, 12 (2012); also available at <http://meetings.aps.org/link/BAPS.2012.MAR.A17.12>.
- ¹⁶R. Garg, A. Senyshyn, H. Boysen, and R. Ranjan, *Phys. Rev. B* **79**, 144122 (2009).
- ¹⁷A. Durán, E. Martínez, J. Díaz, and J. Siqueiros, *J. Appl. Phys.* **97**, 104109 (2005).
- ¹⁸A. Kovalevsky, A. Yaremchenko, S. Populoh, A. Weidenkaff, and J. Frade, *J. Appl. Phys.* **113**, 053704 (2013).
- ¹⁹S. Ohta, T. Nomura, H. Ohta, M. Hirano, H. Hosono, and K. Koumoto, *Appl. Phys. Lett.* **87**, 092108 (2005).